J|A|C|S COMMUNICATIONS

Published on Web 06/08/2009

Control of Bioelectrocatalytic Transformations on DNA Scaffolds

Gilad Piperberg, Ofer I. Wilner, Omer Yehezkeli, Ran Tel-Vered, and Itamar Willner*

Institute of Chemistry, The Hebrew University of Jerusalem, Jerusalem 91904, Israel

Received January 29, 2009; E-mail: willnea@vms.huji.ac.il

Electrical contacting of redox enzymes with electrodes is one of the most fundamental topics of bioelectrochemistry.[1] Different methods for electrically wiring redox proteins with electrodes have been developed, including the immobilization of the proteins in redox-active polymers,[2,3] tethering of redox relays to enzymes,[4] reconstitution of apoproteins on relay-cofactor units,[5] and assembly of enzyme−nanoparticle[6] or enzyme−carbon nanotube hybrids[7] on electrodes. We report on the electrical contacting of redox proteins with electrodes by their spatial organization on DNA scaffolds linked to the electrodes. We show that the structural organization of relay-enzyme components on the DNA scaffold controls the effectiveness of the bioelectrocatalytic processes. These results complement previous studies that have reported on programmed biocatalytic[8] and photocatalytic[9] transformations on DNA scaffolds.

Scheme 1. Electrical Contacting of GOx with an Electrode by the Ordered Hybridization of Ferrocene and GOx on a DNA Scaffold Associated with the Electrode

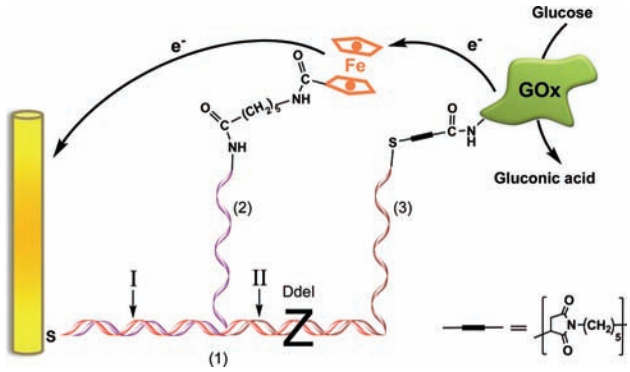

Scheme 1 depicts the bioelectrocatalytic activation of glucose oxidase (GOx) on the DNA scaffold and the generation of an anodic electrocatalytic current. The thiolated nucleic acid (**1**) acted as a scaffold for the organization of the relay-enzyme system. The amine-functionalized nucleic acid (**2**) was covalently linked to ferrocene amidopentyl carboxylic acid succinimidyl ester (Fc), whereas the thiol-functionalized nucleic acid (**3**) was covalently tethered to GOx by the bifunctional cross-linker *N*-(maleimidocaproyloxy)sulfosuccinimide ester. By measuring the absorbance associated with the nucleic acids, we estimated that ∼5 units of (**3**) were linked per protein. The nucleic acids (**2**) and (**3**) include the base-sequence domains I and II, respectively, that enable the directed hybridization of (**2**)−Fc and (**3**)−GOx to the scaffold (**1**). The surface coverage of (**1**) was estimated to be 4.2×10^{-12} mol cm^{-2} using a quartz crystal microbalance (QCM). The surface coverage of (**2**)−Fc was estimated by QCM, and by the coulometric analysis of the Fc redox wave [see Supporting Information (SI)] to be $(3.0 \pm 0.4) \times 10^{-12}$ and $(2.3 \pm 0.3) \times 10^{-12}$ mol cm^{-2}, respectively. The surface coverage of (**3**)−GOx was estimated by QCM and an assay of the activity of the bound enzyme to the electrode (see the SI) to be $(9.4 \pm 0.5) \times 10^{-13}$ and $(6.5 \pm 0.5) \times 10^{-13}$ mol cm^{-2}, respectively. Figure 1 shows the bioelectrocatalytic currents generated by the system in the presence of various concentrations of glucose. Exclusion of the (**2**)−Fc unit from the scaffold eliminated any electrocatalytic currents upon addition of glucose, implying that the ferrocene relay wires the enzyme redox center to the electrode (for the effect of a shorter nucleic acid tether linking the ferrocene unit to the scaffold, see the SI).

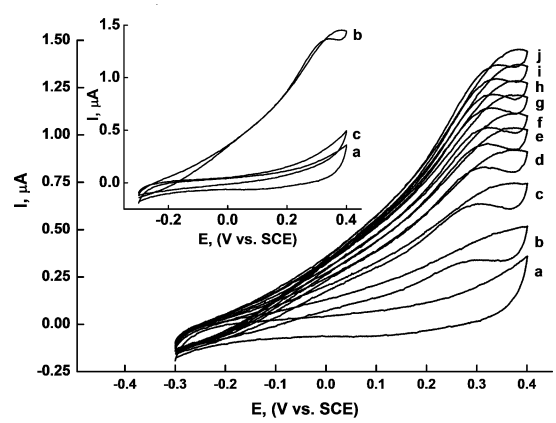

Figure 1. Cyclic voltammograms corresponding to the electrocatalytic anodic currents generated by the ferrocene/GOx electrode in the presence of (a) 0, (b) 20, (c) 40, (d) 60, (e) 80, (f) 100, (g) 120, (h) 140, (i) 160, and (j) 180 mM glucose. Inset: Cyclic voltammograms of the ferrocene/GOx units linked to the DNA scaffold (a) before addition of glucose, (b) after the addition of 180 mM glucose, and (c) after treatment of the system with 2 mg mL^{-1} DdeI in the presence of 180 mM glucose. All of the measurements were recorded in a 0.1 M phosphate buffer (pH 7.4). The scan rate was 10 mV s^{-1}, and the electrode roughness factor was 1.3.

Electrochemical oxidation of the ferrocene units to ferrocenyl cations results in the mediated oxidation of the $FADH_2$ site of GOx and the subsequent oxidation of glucose. Furthermore, the duplex structure between domain II and the scaffold includes the sequence-specific region for cleavage by the endonuclease DdeI. Accordingly, the (**2**)−Fc/(**3**)−GOx assembly that revealed the bioelectrocatalytic oxidation of glucose (Figure 1 inset, curve b) was treated with DdeI, and the bioelectrocatalytic activity of the electrode was examined (curve c). Evidently, the electrocatalytic current was depleted, implying that the biocatalyst was cleaved from the scaffold by the endonuclease. It should be noted that the nonideal shape of the cyclic voltammograms shown in Figure 1 may be attributed to the flexibility of the Fc units linked to the nucleic acid tethers and to partial electrostatic binding of the oxidized Fc to the nucleic acid chains, resulting in a broad domain of formal redox potentials.

For comparison, a system consisting of (**2**)-functionalized GOx and (**3**)-modified ferrocene was assembled on the DNA scaffold (Scheme 2). The surface coverages of (**3**)−Fc and (**2**)−GOx were estimated to be $(3.9 \pm 0.4) \times 10^{-12}$ and $(9.5 \pm 0.4) \times 10^{-13}$ mol cm^{-2}, respectively. Our results indicate that in this assembly, the bioelectrocatalytic oxidation of glucose was blocked (Figure S4 in

10.1021/ja900718m CCC: $40.75

Scheme 2. Nonelectrically Contacted GOx/Ferrocene Configuration on a DNA Scaffold Linked to the Electrode

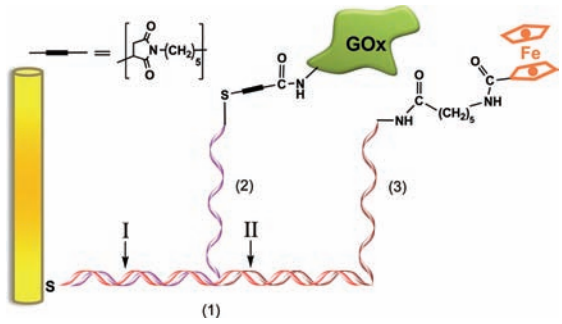

the SI). This is explained by the remote positioning of the ferrocene unit on the DNA scaffold and the consequent screening of the electrical contact between the ferrocene units and the electrode by the GOx positioned close to the electrode. However, the (**2**)−GOx hybridized with the scaffold existed in a biocatalytic configuration, and, upon the addition of diffusional ferrocene carboxylic acid to the electrolyte, the bioelectrocatalytic oxidation of glucose was activated.

The control of bioelectrocatalytic transformations by means of the spatial organization of biomolecules on the DNA scaffold was further demonstrated by activating an electrocatalytic cascade using microperoxidase-11 (MP-11) and GOx as biocatalysts. In one configuration, the (**2**)-modified MP-11 was hybridized with the scaffold at the position adjacent to the electrode, and GOx was positioned at the remote position (Scheme 3).

Scheme 3. Bioelectrocatalytic Reduction of H_2O_2 Generated by GOx Using an MP-11/GOx Cascade Operating on a DNA Scaffold

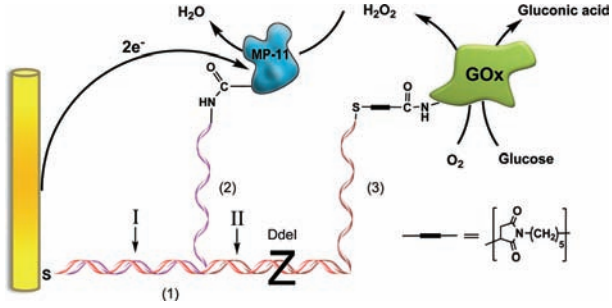

This configuration effectively activated the bioelectrocatalytic reduction of H_2O_2 (Figure 2). In this system, GOx oxidizes glucose by O_2 while generating H_2O_2. The MP-11 electrocatalyzes the reduction of the H_2O_2, giving rise to the electrocatalytic cathodic currents. The MP-11/GOx assembly organized on the DNA scaffold was, then, treated with the endonuclease DdeI. The electrocatalytic activity of the system was substantially lower (Figure 2 inset, curve c vs curve b), indicating that the biocatalyst that generated H_2O_2 was removed from the scaffold. In a further control experiment, the bioelectrocatalytic response of the system that included (**3**)−GOx on the scaffold, in the absence of the mediating MP-11, was examined. Under these conditions, no electrocatalytic current was observed, implying that the reduction of H_2O_2 was indeed electrocatalyzed by MP-11.

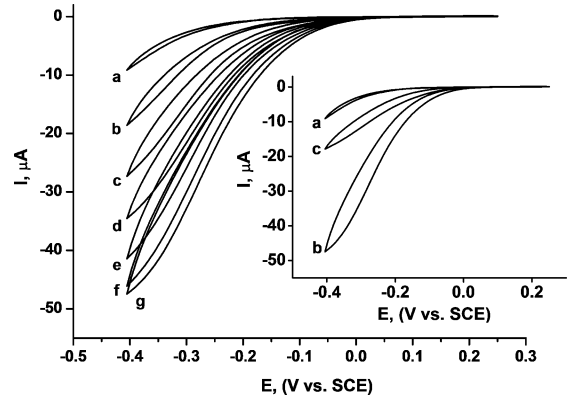

Figure 2. Cyclic voltammograms corresponding to the electrocatalytic cathodic currents generated by the MP-11/GOx electrode in the presence of (a) 0, (b) 20, (c) 40, (d) 60, (e) 80, (f) 100, and (g) 120 mM glucose. Inset: Cyclic voltammograms of the MP-11/GOx units linked to the DNA scaffold (a) before addition of glucose, (b) after the addition of 120 mM glucose, and (c) after treatment of the system with 2 mg mL^{-1} DdeI, in the presence of 120 mM glucose. The measurement conditions were the same as in Figure 1.

The ordering of GOx and MP-11 was further altered by the hybridization of the (**2**)−GOx and (**3**)-functionalized MP-11 on the DNA scaffold (Scheme S1 in the SI). The electrocatalytic currents corresponding to the electrocatalyzed reduction of H_2O_2 were minute (∼10% of the values obtained for the opposite configuration; see Figure S5). These results can be rationalized in terms of inefficient electrical contact of MP-11 with the electrode due to the spatial separation of the peptide and of the insulating effect of the GOx adjacent to the electrode.

In conclusion, the present study has demonstrated that spatial organization of redox-active biomolecules on DNA scaffolds leads to programmed bioelectrocatalytic transformations at electrode surfaces.

Acknowledgment. This research was supported by the Israel Science Foundation and the EC BIOMEDNANO Project.

Supporting Information Available: Figures S1−S6 and Scheme S1. This material is available free of charge via the Internet at http://pubs.acs.org.

References

(1) (a) Gray, H. B.; Winkler, J. R. *Q. Rev. Biophys.* **2003**, *36*, 341. (b) Heller, A. *Acc. Chem. Res.* **1990**, *23*, 128.
(2) (a) Rajagopalan, R.; Aoki, A.; Heller, A. *J. Phys. Chem.* **1996**, *100*, 3719. (b) Gregg, B. A.; Heller, A. *J. Phys. Chem.* **1991**, *95*, 5970.
(3) Heller, A. *J. Phys. Chem.* **1992**, *96*, 3579.
(4) (a) Schuhmann, W.; Ohara, T. J.; Schmidt, H.-L.; Heller, A. *J. Am. Chem. Soc.* **1991**, *113*, 1394. (b) Degani, Y.; Heller, A. *J. Am. Chem. Soc.* **1988**, *110*, 2615. (c) Willner, I.; Riklin, A.; Shoham, B.; Rivenson, D.; Katz, E. *Adv. Mater.* **1993**, *5*, 912.
(5) (a) Zayats, M.; Katz, E.; Willner, I. *J. Am. Chem. Soc.* **2002**, *124*, 14724. (b) Katz, E.; Sheeney-Haj-Ichia, L.; Willner, I. *Angew. Chem., Int. Ed.* **2004**, *43*, 3292. (c) Zayats, M.; Willner, B.; Willner, I. *Electroanalysis* **2008**, *20*, 583.
(6) Xiao, Y.; Patolsky, F.; Katz, E.; Hainfeld, J. F.; Willner, I. *Science* **2003**, *299*, 1877.
(7) Patolsky, F.; Weizmann, Y.; Willner, I. *Angew. Chem., Int. Ed.* **2004**, *43*, 2113.
(8) Niemeyer, C. M.; Koehler, J.; Wuerdemann, C. *ChemBioChem* **2002**, *3*, 242.
(9) Tel-Vered, R.; Yehezkeli, O.; Yildiz, H. B.; Wilner, O. I.; Willner, I. *Angew. Chem., Int. Ed.* **2008**, *47*, 8272.

JA900718M